Conf-740920--10

THRESHOLD PHOTONEUTRON SPECTRA

by

H. E. Jackson

Presented at:

International Symposium on Neutron Capture Gamma Ray Spectroscopy
Petten, Holland, September 2-6, 1974

THRESHOLD PHOTONEUTRON SPECTRA

H. E. Jackson, Argonne National Laboratory

ABSTRACT

Photoneutron spectra in the resolved resonance region near threshold are reviewed as a tool for the study of the neutron capture reaction mechanism. Recent measurements of the photodisintegration of the deuteron near threshold suggest discrepancies with the elementary model of the reaction. Data for nuclei in the mass region $A \approx 50-60$ contain partial width correlations and non-resonant reaction components characteristic of channel capture. Other nuclear structure effects in the form of intermediate structure and partial width correlations for heavier nuclei are also discussed. Photon strength functions for E1 and M1 radiation resulting from measurement of threshold photoneutron spectra are compared with data from other sources and theoretical predictions. Intense p-wave photoneutron emission by the Pb isotopes indicates the presence of a magnetic dipole giant resonance whose integrated strength is close to the theoretical limit.

I. Introduction

To a considerable extent, the continuing interest in threshold photoneutron reactions is a result of their value as a tool in the spectroscopy of highly excited nuclear states. However, most of our knowledge in this area has come from studies of particle induced reactions, and so we quite naturally discuss the radiative process as a capture reaction and cast our theoretical models in terms of capture mechanisms. For this reason it is convenient to view photoneutron emission as "inverse capture" and relate the results to our understanding of the capture reaction. I would like to discuss this field from that perspective. Inasmuch as the most basic capture reaction is neutron capture in hydrogen, it is appropriate to introduce the subject with a brief discussion of the inverse process, i.e. the photodisintegration of the deuteron in the threshold region. The main body of the paper will be a review of our present experimental understanding of threshold photoneutron spectra, with emphasis placed successively on three topics — reaction mechanisms, E1 radiative strength, and the M1 giant dipole resonance.

The simplest and the most basic threshold measurement one can make is the photodisintegration of the deuteron. At threshold, the cross section is well

established through measurements of the inverse n-p capture cross section, and above energies of 2.5 MeV measurements using a radioactive monochromatic photon sources have been made. The energy region between these points continues to be of interest because of an apparent enhancement of the n-p cross section by about 10% at thermal energies and unresolved discrepancies between the observed and theoretical angular distributions of the photonucleons. Riska and Brown[1] have recently demonstrated that the 10% discrepancy in the thermal value can be accounted for in terms of the effect of meson exchange currents.

In the elementary theory of the deuteron, the photodisintegration process is assumed to proceed solely through $^3S \rightarrow {}^1S$ magnetic dipole and the $^3S \rightarrow {}^3P_{0,1,2}$ electric dipole transitions. In the threshold region, the amplitudes for these processes can be calculated accurately using the zero range central force approximation. Typical results are shown in Fig. 1. Very close to threshold the photomagnetic process dominates, but very quickly the photoelectric reaction becomes the major reaction mode. Because the singlet and triplet states do not interfere in this approximation, the angular distribution of the photoneutron is given by:

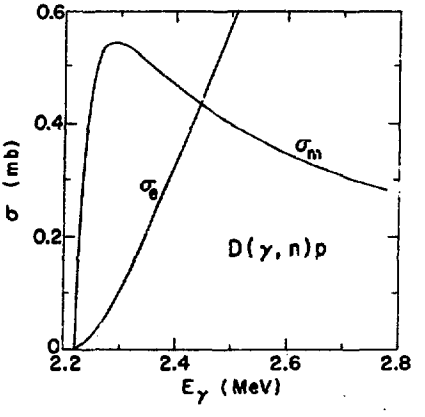

Fig. 1. Photoelectric and photomagnetic cross sections of the deutron near threshold.

$$\frac{d\sigma}{d\Omega} = a + b \sin^2 \theta_n \qquad (1)$$

where θ_n is the angle between the photoneutron and the incident photon in the center of mass system. The constants a and b are directly related to the total total photomagnetic and photoelectric cross sections in the ration $\sigma_m/\sigma_e = 3a/2b$. Deviations from the simple model which result in departures from the angular distribution of eq. 1 would be expected to be most pronounced in the region where σ_m and σ_e are comparable, i.e. about 100-200 keV above threshold. We are currently studying the photodisintegration reaction at ANL in the threshold region by irradiating a deuterium target with low energy pulsed bremsstrahlung and measuring the photoneutron

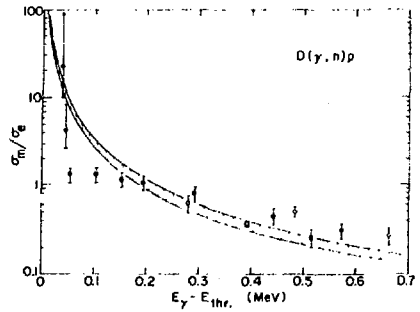

Fig. 2. The observed ratio of the photomagnetic to photoelectric cross section of the deutron near threshold. Open circles are older data (see ref. 2).

energy spectrum by neutron time-or-flight at 90° and 135° to the incident photon beam. Our results are shown in Fig. 2, where they are compared with theoretical prediction and previously measured values.[2] I must emphasize that these are our first results and that the measurement is a continuing. The data shown is the ratio, σ_m/σ_e obtained by assuming the elementary model of the deuteron. The shaded region in the figure indicates the values implied by a reasonable choice of effective range parameters. While the points at higher energy are in reasonable agreement with the older measurements, deviations from the theoretical values are quite clear-values are high at higher energies and too low near threshold. While it is too early to reach any definitive conclusion, it is of interest to inquire into possible explanations for anomalies in the angular distribution of the photoneutron. The data suggest that the assumption of an angular distribution of the form eq. 1 is not valid. Certainly any final state interaction leading to spin mixing would violate this assumption and lead to an interference term which could account for the angular distribution we observe. Alternatively, such mixing could be produced by a momentum dependent component in the nucleon potential, as has been suggested recently by Breit and co-workers.[3] In either case, the resulting interference would explain the long standing discrepancies in the threshold region in the reported values of the relative strength of the photomagnetic and photoelectric disintegration and necessitate a re-analysis of the data in terms of a more complex angular distribution. It is clear that future measurements of angular distribution should cover such a range as to place definite limits on the existence of an interference asymmetry around 90°.

In contrast to the deuteron, the photoneutron spectra from complex nuclei are complicated by the existence of many exit channels leading to residual excited states in the daughter nucleus. Figure 3 shows schematically the total absorption cross section for a typical medium mass nucleus. Close to threshold, where

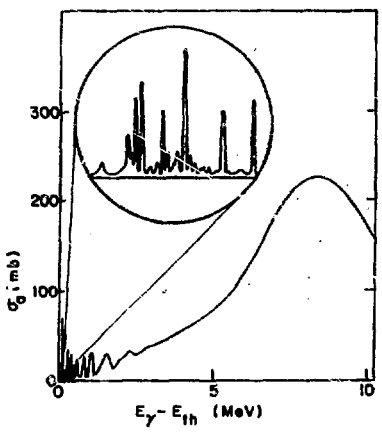

Fig. 3. Schematic plot of the photoabsorption cross section in the region above neutron threshold for a nucleus with A ≈ 60.

only a few particle channels are open, the total resonance widths are much less than the resonance spacings and the structure in the photoabsorption cross section can be interpreted in terms of individual highly excited nuclear states. The key to measurements in the threshold region is the use of bremsstrahlung radiation with a precisely defined end point energy to excite these states. For example, if $(E_\gamma - E_{th})_{max}$ is less than the first excited state of the daughter nucleus, photoexcitation is limited to a small band of excited levels just above the neutron binding energy, which can decay by neutron emission only through transitions to the ground state of the daughter nucleus. In the typical experiment nanosecond pulses of bremsstrahlung are used to excite the levels of interest and the resonance structure is observed with extremely high resolution characteristic of neutron time-of flight measurements. A typical time spectrum is shown in Fig. 4 for a nucleus which will be discussed later. In such a spectrum the resonance yield is proportional to the product $\Gamma_{\gamma_0}\Gamma_n/\Gamma$ where Γ_{γ_0} is the ground state radiation width.

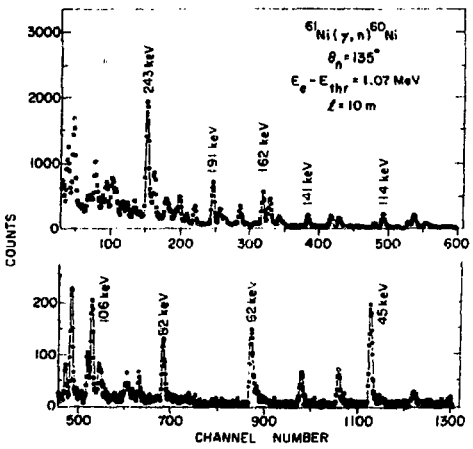

Fig. 4 Photoneutron time-of-flight spectrum for ^{61}Ni(γ,n).

Because $\Gamma_n/\Gamma = 1$ is a good approximation in the threshold region, the resonance yield in such a measurement is a direct estimate of the ground state radiation width. Therefore, by studying the detailed properties of individual levels in the resolved region, one obtains individual ground state radiation widths as well as average quantities such as the photon strength function. In addition, the photoneutron angular distribution gives information on the resonance spins and parities. With this technique, large experimental samples of resolved resonances of a given J^π can be obtained for many targets. Of course, there are variations in this basic idea in which the end point energy is successively varied to permit an extension of the region over which the ground state radiation widths can be derived from the experimental spectrum.

II. Reaction Mechanisms

Just as in neutron induced reactions, much information about the reaction mechanism for radiative transitions can be obtained by studying the characteristics of the photoneutron resonance structure. The relative magnitude of resonant and non-resonant reaction can be estimated from the analysis of resonant shapes, the importance of single particle effects can be estimated by observation of correlations between various resonance parameters, and the existence of simple, intermediate and doorway configurations in the reaction mode can be associated with intermediate structure in the distribution of resonance strength. Let us consider the data available from these points of view.

Channel Capture

Non-resonance reaction amplitudes can be established in photoneutron spectra directly from the asymmetry produced by the interference between the reaction amplitude due to an isolated resonance, and the underlying non-resonant amplitude. The threshold photoneutron technique is particularly well suited for measuring resonant shapes because of the absence of significant multiple scattering of the emerging neutron. This fact is demonstrated by recent data obtained for a resonance at 12 keV in ^{61}Ni shown in Fig. 5. The state in ^{61}N is of particular interest because analysis of earlier data [4] has suggested the existence of sizeable non-resonance reaction amplitudes in the mass region $\sim A = 50-70$. As the time-of-flight spectrum indicates, in this particular case any interference asymmetry is extremely weak. A detailed analysis of the shape gives $\sigma_{nr} = 12\ ^{+20}_{-10}$ μb, a value which is just at our limit of detection. It is important to note the absence of any inherent instrumental asymmetries in this measurement.

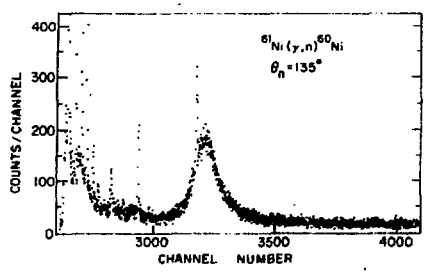

Fig. 5. Photoneutron time-of-flight spectrum for ^{61}Ni in the region of the 11.7 keV resonance.

In contrast to the result for ^{61}Ni, we have observed a very strong interference effect in the 91 keV resonance in ^{53}Cr(γ,n). The data is shown in Fig. 6. A time-of-flight spectrum is shown in the inset. A very pronounced low-energy tail is quite clear in the shape of the 91 keV resonance as observed in this spectrum. The result of a shape analysis in terms of a non-resonant background cross section interfering with a resonant amplitude is shown in the main part of the figure. In this case, the best fit to the data is obtained for a value $\sigma_{nr} = 200\,\mu b$. Two comments must be made. First, this resonance is clearly not an isolated level; however, examination of the parameters for the nearby resonances indicated that contributions from these states cannot explain the observed asymmetric shape. Second, the unexplained structure on the low-energy should of the 91 keV level can be attributed

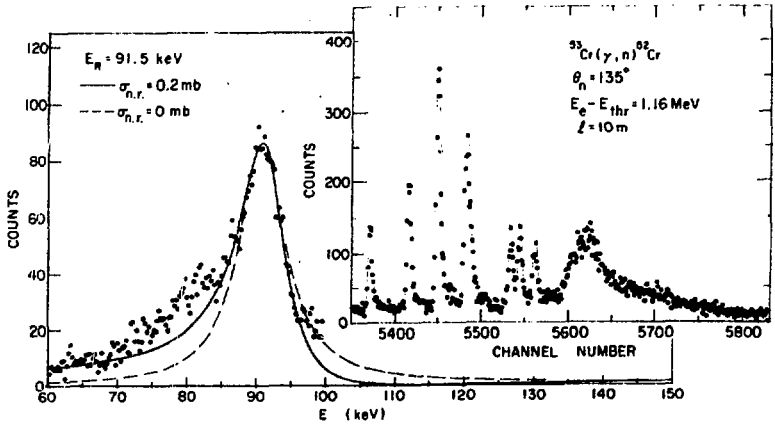

Fig. 6. Shape analysis of 91 keV photoneutron resonance in ^{53}Cr. Inset shows the time-of-flight spectrum in the region of the resonance.

to several levels too weak to give rise to a significant interference effect. Such a conclusion is implied by failure to observe these levels in the total neutron or capture cross sections of ^{52}Cr. Thus, in spite of the complications of this case, it appears that 200 μb is a reasonable estimate for the non-resonant cross section near 100 keV.

As you will remember, the Cr-Ni mass region is of particular importance in the theory of channel capture. In the original Lane-Lynn formalism,[5] radiative capture was resolved into an ordinary resonant compound nucleus "internal capture" term and a "channel capture" term arising from contributions to the reaction amplitude in the region outside the nuclear surface. The channel component was resolved in the single level approximation into a Breit-Wigner component distinguishable from the normal compound term only because its strength is determined by the reduced width of the initial and final states:

$$U_{res}(E) = ie^{i\phi_c}\Gamma_{\lambda c}^{\frac{1}{2}}\ \delta\Gamma_{\lambda\gamma f}^{\frac{1}{2}}/(E_\lambda - E - i\Gamma_\lambda/2) \qquad (2)$$

$$\delta\Gamma_{\lambda\gamma f}^{\frac{1}{2}} \approx k\ \frac{E\gamma}{\hbar c}^{\frac{3}{2}}\ \theta_{fc}\,\theta_{\lambda c'}$$

and a non-resonant potential capture term again proportional to θ_{fc}, the final state reduced width:

$$U_{pot}(E) \approx k'\theta_{fc}/\sqrt{\Sigma}^{\frac{1}{2}} \qquad (3)$$

Because of this dependence on θ_{fc}, the channel component is commonly interpreted as a direct reaction.

When the channel contribution is significant, strong correlations between the neutron width and the partial radiation widths should occur. In addition, the non-resonant component arising from potential capture can be significant. Lane[6] has observed that the channel capture could account for almost all the radiative strength of high energy E1 transition for nuclei below A ≈ 100, and more recently in detailed calculations Lubert et al.[4] proposed that channel capture should dominate in the chromium-nickel region. The threshold photoneutron spectra can be used to explore this hypothesis for ground state transitions by measuring the radiation widths in this mass region for s-wave resonances which are excited by E1 absorption. Fortunately for targets of major interest, values of Γ_n for the s-wave resonances are well established in the total cross-sections observed for the daughter nuclei. However, the

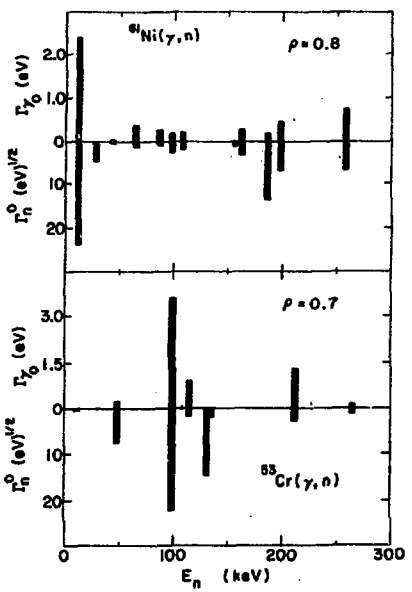

Fig. 7. Comparison of ground state radiation widths and reduced neutron widths of resonances in ^{53}Cr and ^{61}Ni.

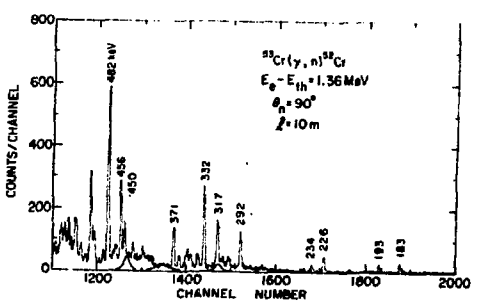

Fig. 8. Photoneutron time-of-flight spectrum observed with a proton recoil detector for a ^{53}Cr target. Several known unresolved broad s-wave levels are indicated.

observation of these levels in (γ,n) spectra has proved to be extremely difficult. Because of the enhanced sensitivity of the threshold technique to p and d wave resonances, broad s-wave resonances can easily be lost under the structure of levels with $\ell > 0$. this is illustrated in the history of measurements of the resonance shown in Fig. 6. In the earliest measurements of this region,[7] this s-wave resonance was not even identified. In our earliest published results,[8] the level was isolated but its yield was badly underestimated. Only recently, as a result of our increased experimental sensitivity, have we been able to obtain a reliable estimate of the strength and shape of this resonance.

Using the new data, we have completed the correlation analysis shown in Fig. 7. ^{57}Fe was excluded from this study because it is well known that the parentage of the ground state of ^{57}Fe is an excited state of ^{56}Fe, and as a result no strong effects of channel capture should occur. The data for ^{53}Cr cover only that region in which the resonance structure was well resolved. The result, p = 0.68, although statistically significant, is not conclusive. The analysis was extended to higher energy with the data of Fig. 8 which illustrates the difficulty in observing s-wave levels in the presence of a strong

p-wave M1 component. In this case, it was only possible to explore the consistency of the data with a strong correlation by assigning to the broad s-wave levels known to exist at higher energies strength indicated in the figure which are consistent with the shape of the (γ,n) spectrum in the region. In this manner, a sample of 14 resonances in ^{53}Cr gave a strong correlation of $\rho = 0.71$.

A correlation analysis of resolved resonances in ^{61}Ni is shown in Fig. 7; again there is a statistically significant correlation, but here also the correlation results predominantly from a single resonance strong both in the neutron and photon channel. However, a joint analysis of these two populations using only the data of Fig. 7 does give a definitive result. The correlation coefficient for the joint population is $\rho = 0.76$. The probability of obtaining such a result from an uncorrelated population is less than 1%. Thus, these data confirm the prediction of the channel theory and in addition, support the suggestion of Block and coworkers[9] that a strong correlation which they observed between the total radiation width and neutron width for nuclei in this mass region can be explained in terms of partial radiation width correlations.

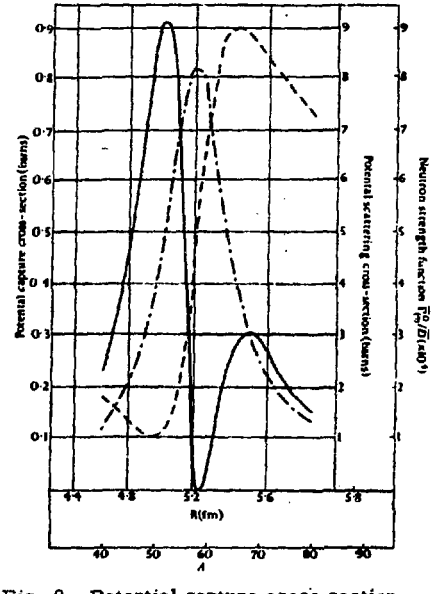

Fig. 9. Potential capture cross section (solid line) near A = 60. Also shown are the potential scattering cross section (dashed line) and neutron strength function (dot-dash curve).

The large non-resonant cross section observed for ^{53}Cr can also be understood as a channel effect. This cross section is to be compared with a value of 0.88 μb which results from the strong coupling calculation of the "hard sphere" or "potential" capture cross section for ^{53}Cr. The trend observed in calculations using an intermediate coupling model[10] indicate that a more accurate calculation would probably be closer to the 200 μb value observed in the photoneutron measurements.

Perhaps of more significance is the observation of a small non-resonant cross section in the same mass region in ^{61}Ni. This is precisely the trend observed by Lane and Lynn in their original intermediate coupling model. Fig. 9 shows the σ_{pot} which was obtained in this approximation. The rapid variation with mass was associated with the

maximum and minimum in the potential scattering cross section in the mass region. ^{61}Ni lies right in the minimum in σ_{pot} indicated by this calculation, while ^{53}Cr is in the region of strong potential capture exactly as the photoneutron experimental data indicate. In conclusion, the photoneutron resonance structure for this mass region displays precisely those characteristics that one associates with channel capture.

A reaction mechanism closely related to channel capture, the valence model and valence transitions, have been extensively reviewed by earlier speakers. In view of this discussion, I wish only to mention that dramatic correlations between Γ_n and $\Gamma_{\gamma o}$ have been observed in the study of ^{91}Zr (γ,n) by Toohey and Jackson.[11] In this case, the effect can be attributed to single particle valence transitions between the d 5/2 neutron orbital and the p 3/2 unbound resonances. Toohey's results indicate that valence transitions account for a major portion of the E1 transition amplitude in the threshold region for this target.

Intermediate Structure

The other aspect of photoneutron resonance structure which has received continuing attention is the search for intermediate structure and its interpretation in terms of nuclear structure features peculiar to a particular nucleus or local mass region. A great deal of effort has focused on the search for "common doorway" phenomena, i.e. local concentrations of resonance strength which appears simultaneously in more than one channel leading to the same intermediate state. In such cases, the common doorway is a particularly simple nuclear configuration with large matrix elements in both channels which dominate the reaction.

Convincing evidence for a common photon doorway, albeit in a light nucleus, has been observed in our Argonne measurement of the threshold cross section of ^{29}Si. The results are shown in Fig. 10. Newson has proposed[12] a neutron doorway in ^{29}Si based on a localization of p-wave neutron strength near 800 keV. We find a similar concentration in the photon channel. From measurements of the neutron angular distribution, we can show the resonances to be mostly $J^{\pi} = \frac{3}{2}^{-}$. Although the sample size is small, a striking correlation is evident. Even when corrected for the most recent high resolution capture data[13] on ^{29}Si, we obtain a correlation coefficient for the sample of $\rho = 0.8$. We have suggested that these results should be interpreted in terms of a common doorway corresponding to a 2 p $\frac{1}{2}$ neutron coupled to a ^{28}Si core. The excitation energy of the 2 s $\frac{1}{2} \rightarrow 2\,p\frac{3}{2}$ single particle transition is expected to be approximately 10 MeV for nuclei in this region, just above the threshold in ^{29}Si.

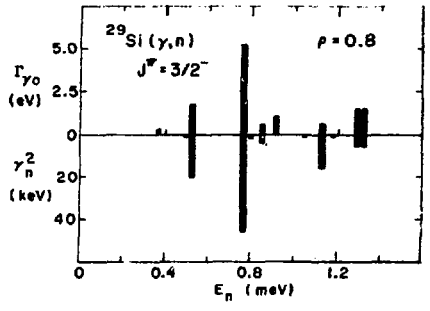

Fig. 10 Ground state radiation widths and reduced neutron widths for resonances in ^{29}Si.

The ^{207}Pb nucleus is also of interest in this regard. In studies of the total neutron cross section of ^{206}Pb, Farrel observed a sharp concentration of strength[14] which was interpreted in terms of a doorway state in ^{207}Pb, whose parent was a single $\frac{1}{2}$ + resonance in ^{208}Pb near 500 keV. Initially, this doorway was interpreted in terms of a 2p-1h excitation, which suggested that the neutron doorway should be common to the photon channel and that the partial widths should be strongly correlated. In early efforts to confirm this prediction, the photoneutron spectrum of ^{207}Pb was studies and indeed, the expected correlations were observed[15] with a strength corresponding to a correlation coefficient $\rho = 0.44$. For some time thereafter, this case was considered one of the best examples of a common doorway. However, recently a more detailed examination by Beres and Divadeenam[16] has indicated that the conjectured 2p-1h states occur too high in excitation and imply too large an integrated strength. Instead, they find a reasonable candidate to be a particle-vibration state described as a 2g 9/2 neutron coupled to a 4+ vibrational state of the ^{206}Pb core. In this view, the radiative transition would not be particularly enhanced by the presence of such a doorway, and the reported correlation would be unexpected. In addition, studies of capture in ^{206}Pb[17] indicate that the resonance structure of ^{207}Pb was more complex than Baglan et al. could have realized. With these developments in mind, Medsker[18] has re-examined the threshold spectrum of ^{207}Pb with improved resolution and has also measured the angular distribution. From this data for 1^+ resonances (Fig. 11) he found a correlation coefficient $\rho = 0.1$. Both this value of ρ and the visual indication from the bar graph are consistent with no correlation. Thus the new data support

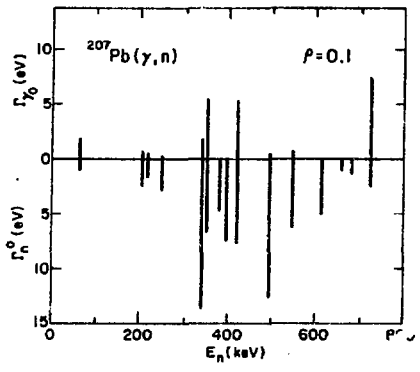

Fig. 11. Comparison of radiation widths and reduced neutron widths of resonances in ^{207}Pb.

the particle-vibration doorway interpretation of Beres and Divadeenam in preference to the view that there is a common doorway.

Structure corresponding to a simple doorway state has been observed in the M1 excitation of p-wave resonances in ^{57}Fe.[19] The data are shown in Fig. 12. Spins and parities were assigned from angular distribution results and comparisons with total neutron cross section data for ^{56}Fe. The assignments indicate very sharp concentrations of strength for both $\frac{1}{2}^-$ and $\frac{3}{2}^-$ resonances. The integrated M1 strength is not unusually large. However, although about thirty $\frac{3}{2}^-$ levels are expected between 0 and 300 keV, all the M1 strength for this group appears to be concentrated in resonances at 224 and 225 keV. Similarly, for $\frac{1}{2}^-$ resonances below 600 keV, almost all the M1 strength is concentrated in the resonance at 606 keV. A statistical analysis indicates that the frequency with which such a distribution can be generated by random fluctations is $\lesssim 10^{-3}$. Because the calculated difference between the filled $f_{\frac{7}{2}}$ orbital and the $f_{\frac{5}{2}}$ orbital ~8 MeV in this mass region, the intermediate structure could be interpreted in terms of a two-quasi particle doorway consisting of a $(f_{\frac{5}{2}})(f_{\frac{7}{2}})^{-1}$ particle-hole pair coupled to the ^{57}Fe ground state. A spin-flip transition of an $f_{\frac{7}{2}}$ nucleon would generate a particle-hole pair which can couple to ^{57}Fe to give rise to doorways in both the $\frac{1}{2}^-$ and $\frac{3}{2}^-$ channels. The sharpness of the structure suggests that the damping widths of the doorway states are so small that the strength of each doorway is spread over only a few resonances.

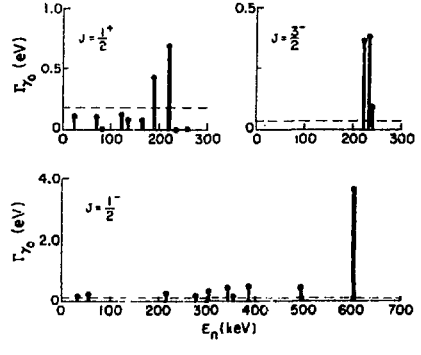

Fig. 12. Ground-state radiation widths Γ_{γ_0} for resonances in ^{57}Fe.

Finally, let me comment that we will discuss below in connection with the M1 photon strength function what might be the most dramatic example of a photon doorway, namely the giant M1 resonance as observed in the lead isotopes.

Nonresonant Processes in ^{208}Pb

Before leaving the subject of reaction mechanisms, it is appropriate to comment on the continuing controversy over the existence of an anomalous non-resonant cross section in ^{208}Pb. This problem arose as a result of early photoneutron studies of the 41 keV resonance in ^{208}Pb(γ,n) which indicated a gross interference asymmetry. The effect was explained by postulating an interfering background amplitude far in excess of that expected from direct processes. However, subsequent studies of neutron capture in ^{207}Pb in which the same state was studied showed an equally anomalous total absence of any non-resonant reaction. However, this anomaly appears to have been reconciled by new photoneutron data[20] which are included in Table 1.

TABLE I. Comparison of calculated and observed background cross sections for ^{208}Pb(γ,n)^{207}Pb. The values corresponding to a $\sqrt{E_n}$ extrapolation of the thermal (γ,n) cross section are given in the fourth column. The results of a calculation discussed in the text are given in the last column.

E_n (keV)	Experimental σ_{bg} (n,γ) (mb)	Experimental σ_{bg} (γ,n) (mb)	Calculated σ_{bg} Extrap. (mb)	Calculated σ_{bg} (γ,n) (mb)
0.025×10^{-3}	709 ± 10	0.0012	0.0012	0.0012
1.95	3.2 ± 1.2	0.45 ± 0.16	0.34	0.41
25	0.5	0.9 ± 0.2	1.2	1.01
41	. . .	$1.3^{+2.7}_{-0.7}$	1.5	1.15

For original references see H. E. Jackson, Phys. Rev. C 9, 1148 (1974).

Calculated and observed background cross sections are compared at the four energies where measurements are available. Values corresponding to a $\sqrt{E_n}$ extrapolation of the thermal (γ,n) cross section are given in the fourth column. However, since the thermal cross section is much larger than estimates

of direct capture, these figures do not explain the origin of the σ_{bg} and 41 keV. To explore this point, we have calculated the value of σ_{bg} expected to result from constructive interference among the reaction amplitudes arising from the neighboring strong resonance at 255 keV, from the bound level at E_x = 7325 keV, and from the expected direct capture cross section. The results of this calculation, given in the last column of the table 1, agree well with the experimental values. The result illustrates that the observed background cross section can be explained in terms of the known resonance structure of ^{207}Pb plus a normal direct reaction component without recourse to anomalous non-resonant processes. Finally, for these recent experiments both the neutron and photon induced reaction results are in agreement.

III. Electric Dipole Transitions

Another property of photoneutron spectra which is of major importance in understanding radiative transitions is, of course, the average strength of the resonance structure. This feature is conveniently described in terms of the photon strength function, $S(Mp) = \langle \Gamma_{\gamma i} \rangle / D$ for the various multipoles, Mp. The proposition that the E1 strength function can be described in terms of the giant dipole resonance model as developed by the Brink hypothesis and the Axel formulation has been reviewed in earlier talks at this symposium. However, in the case of threshold photoneutron spectra, the relationship of the E1 strength to this model is even less ambiguous, since one is measuring directly the tail of the giant dipole resonance. Let us recall that Axel[21] has used a parameterization of the giant dipole resonance that is applicable to a wide range of nuclei in order to devlop the relationship for the photon strength function which is expected to be accurate in the threshold region:

$$\langle \Gamma_{\gamma o}(E1) \rangle / D = 6.1 \times 10^{-15} E_\gamma A^{8/3} \qquad (4)$$

where E_γ is in MeV.

In Fig. 13 we have presented a summary comparison of E1 photon strength functions parameterized in terms of the giant dipole model, with the prediction of Axel. The solid line is his prediction. These data include results from measurements of average capture spectra, resonance capture spectra and threshold photoneutron spectra. In compiling these data, we required that the number of resonances studied in any measurement be sufficient to suppress the uncertainty imposed on the data by Porter-Thomas fluctuation. For this reason, there are fewer data points than have been included in earlier compilations. The results are very interesting. The strength functions obtained from the threshold measurements fit very

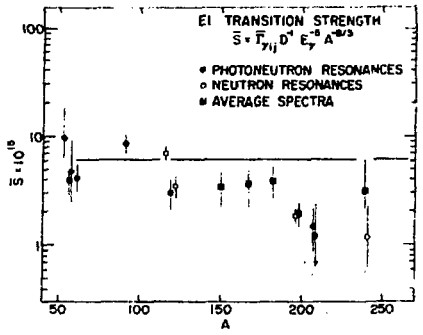

Fig. 13. Average values of the E1 transition strength. The solid curve is the prediction of the giant dipole resonance model (eq. 4).

nicely into the trends observed with the results obtained using the other experimental techniques. However, the overall agreement with the Axel prediction is poor. In the mass region between 150 and 250, the giant dipole model badly overestimates the E1 strength. Perhaps we should not be surprised at this, since only the order of 1% of the total E1 strength as given by the classical dipole sum rule is expected to occur below threshold. The Brink-Axel treatment may simply not be capable of describing such detail. In fact, there are good reasons to doubt that the Lorentzian shape is a valid parameterization of the dipole strength in the wings of the giant resonance.

In view of this poor agreement we can regress a bit and compare the same data with a single particle estimate as is done in Fig. 14. The value indicated here by the heavy black line has been obtained by using the mass and energy dependence characteristic of the Weisskopf single particle value in a calculation in which the dipole matrix element is constrained so that the resulting strength function satisfies the classical dipole sum rule for $A \approx 160$. The quantity plotted is actually the photon strength function divided by the energy and mass dependence of the single particle estimate. Clearly, the prediction based on the dipole sum rule predicts values much too large. If we arbitrarily decrease the single particle estimate by a factor of 3.5, we obtain the dotted curve which agrees with the data at least as well as the Brink-Axel model. Once can speculate that

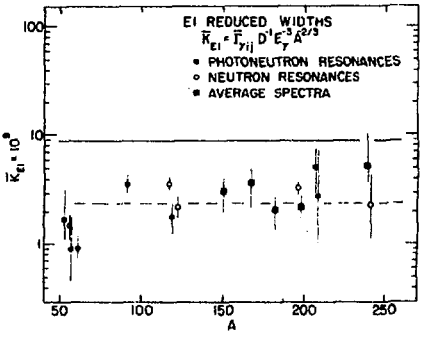

Fig. 14. Average values of E1 reduced widths. The solid line is the prediction based on a normalization according to the dipole sum rule. The dotted line represents an arbitrary normalization.

the single particle model may be more appropriate, if the transition strength in the threshold region somehow arises from the residue of single particle strength which is decoupled from the giant dipole resonance. In any case, the one positive aspect of this problem is that the quality and quantity of data on the electric dipole strength function is growing, and the trends emerging do indicate that a more refined model is appropriate.

III. M1 Transitions

Speculation on the existence of a giant M1 resonance goes back almost a decade,[22] and in spite of this the data on the M1 strength function has remained fragmentary and inconclusive. The M1 resonance is expected to occur in those nuclei for which one spin-orbit partner of a shell model level lies just below the Fermi surface. For such nuclei the M1 strength should be strongly enhanced at those energies corresponding to the spin-flip excitation of a nucleon from the filled to the empty spin-orbit partner. The ideal nucleus for observing such an effect is ^{208}Pb, in which the M1 transitions are expected to result from spin-flip transitions between the i 13/2 and i 11/2 neutron orbits, and between the h 11/2 and h 9/2 proton orbits. In threshold studies of this nucleus, the Livermore group found strong evidence for a giant M1 resonance at an excitation of 7.8 MeV[23]. Their values of $\Gamma_{\gamma 0}$ for $\frac{1}{2}^+$ resonances are shown in Fig. 15. Surprisingly, the integrated strength of this group of resonances was estimated to be at 50.8 eV. This is about 5 Weisskopf units and accounts for at least half of the maximum strength expected for this excitation. The authors interpreted the observed structure in terms of the collective effect of nucleon in the i 13/2 and h 11/2 shells, i.e. these orbitals constitute a collective doorway. Unfortunately, later measurements at ANL[24] indicated that the angular distributions measured in the initial experiments do not provide a unique spin- and parity assignment for levels above 500 keV because of possible admixtures of s- and d-wave neutron decay of 1^- states. The new data imply that only 20 eV of this strength could be assigned with certainty. Further confusion has been created by recent measurements of the

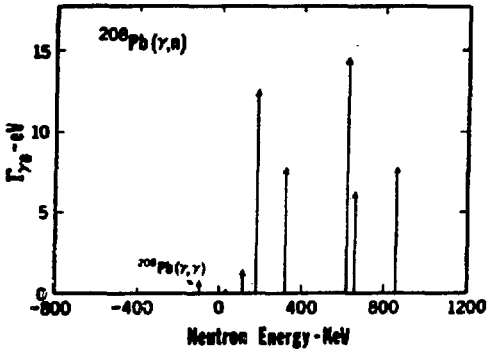

Fig. 15. Ground-state radiation widths for probable 1^+ resonances in ^{208}Pb.

total cross section for ^{207}Pb which indicate that the parity assignments for the strong levels at 181 and 318 keV may be incorrect.

In view of these problems it is a natural to explore alternative targets. Presumably such a giant M1 resonances should manifest itself in all the Pb isotopes at the same excitation. In ^{207}Pb, spin and parity assignments should be less ambiguous since the channel spin for the neutron decay is uniquely determined by the J^{π} of the initial state. We have taken advantage of this fact in measurements of ^{207}Pb(γ,n)[18], and indeed we find that the resonance structure is dominated by M1 photoexcitation. Figure 16 shows a histogram of the distribution of radiative strength among levels whose angular distribution indicate a magnetic dipole excitation. Although the population does include a possible contamination of 1^+ resonances above 718 keV, the data suggest an envelope of M1 strength centered at an energy of approximately 600 keV. In spite of the complication imposed by possible M1 + E2 admixtures, the measured angular distributions enable us to set a lower limit of 125 eV on the integrated strength of M1 resonances in the threshold region. We have considered interpretation of the ^{207}Pb results in terms of a weak coupling model consisting of the p 1/2 hole coupled to a ^{208}Pb core. In this approximation of M1 integrated strength in ^{207}Pb should be twice that ^{208}Pb. Thus our data support the original assertion of the Livermore group that at least 50 eV of M1 strength occurs near threshold in ^{208}Pb. These data also agree well with detailed calculations in ^{208}Pb based on Hamada-Johnston potential,[25] which predicts an M1 giant resonance at 7.5 MeV. The calculated width is approximately 79 eV; however if the effects of core polarization in the ground state of ^{208}Pb should be important, this value could be reduced to approximately 61 eV. In any case in the lead isotopes the Giant M1 resonance appears firmly established by the threshold photoneutron measurements.

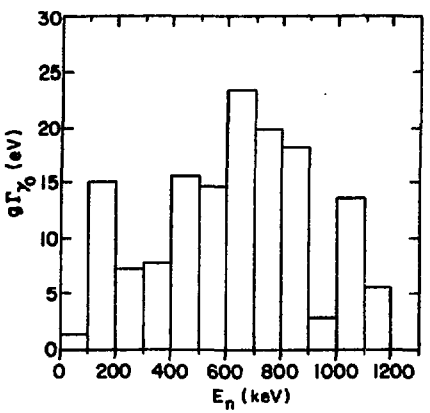

Fig. 16. Histogram at the values of $g\Gamma_{\gamma_0}$ for resonances in ^{207}Pb excited by M1 transitions.

Elsewhere in the periodic table is quite another matter. On the basis of the spin-flip mechanism, one would expect similiar M1 enhancement for nuclei

in the Zr region arising from the g 9/2 → g 7/2 neutron transition; in the Sn region from the g 9/2 → g 7/2 proton transition; and in the Ba region corresponding to h 13/12 → h 11/12 transitions. Unfortunately, for every experiment indicating the observation of such enhanced M1 strength in one of these regions, there is a subsequent experiment whose findings are inconsistent with the earlier data. For this reason it does not seem appropriate to comment on specific measurements. Instead, the experimental data from the photoneutron measurements are summarized and compared in Fig. 17 with other measurements in the threshold region. For the most part the data are consistent with the earlier suggestion of Bollinger:[26]

$$\langle \Gamma_{\gamma i}(M1) \rangle / D \approx 18 \times 10^{-3} \qquad (5)$$

This is ten to twenty times the single particle value. We have already discussed the evidence for enhancement above this value for the lead isotopes. There is also evidence for strong M1 transition in the Ru isotopes from the recent resonance capture results of Chrien and co-workers[27] and evidence for an inhibition of M1 transitions in the Au-Ta region. However with the exception of the Pb isotopes it has not been possible to establish a relationship between nuclear structure and the observed values of the M1 strength function nor to justify the background value which characterizes many nuclei.

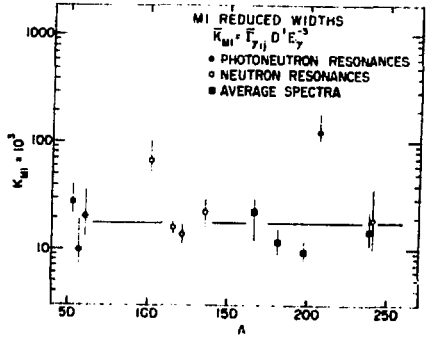

Fig. 17. Average values of M1 reduced widths. The solid line corresponds to eq. 5.

Clearly the M1 giant dipole state is one of the major unsolved problems in radiative neutron reactions. A major objective of future experiments should be a systematic study of the M1 strength over the periodic table and to search for significant departures from the empirical background data which characterizes the limited data avaliable.

In closing I would like to suggest that the study of photoneutron spectra in the threshold region is coming of age and we can expect major contributions to our understanding of neutron capture reactions.

References

1) D. O. Riska and G. E. Brown, Phys. Letters 38B (1972) 193
2) L. Hulthe'n and B. C. H. Nagel, Phys. Rev. 90, (1953) 62
3) G. Breit and M. L. Rustgi, Nucl. Phys. A161,(1971) 337
4) M. Lubert, N. C. Francis, and R. C. Block, Nucl. Phys. A, in press
5) A. M. Lane and J. E. Lynn, Nucl. Phys. 17, (1960) 563
6) A. M. Lane, Ann. Phys. (N.Y.) 63, (1971) 171
7) R. J. Baglan, C. D. Bowman, and B. L. Berman, Phys. Rev. C3, (1971) 672
8) H. E. Jackson and E. N. Strait, Phys. Rev. C4, (1971) 1314
9) R. C. Block, R. G. Stieglitz, and R. W. Hockenbury, Nucl. Phys. A163,
10) A. M. Lane and J. E. Lynn, Nucl. Phys. 17, (1960) 586
11) R. E. Toohey and H. E. Jackson, Phys. Rev. C9, (1974) 346
12) H. W. Newson, in Statistical Properties of Nuclei, ed. J. B. Garg (Plenum, New York, 1972) p. 309
13) B. J. Allen and R. L. Macklin, to be published
14) J. A. Farrel, G. C. Kyker Jr., E. G. Bilpuch, and H. W. Newson, Phys. Letters 17, (1965) 286
15) R. J. Baglan, C. D. Bowman, B. L. Berman, Phys. Rev. C3, (1971) 2475
16) W. P. Beres and M. Divadeenam, Phys. Rev. Letters 25 (1970) 596
17) B. J. Allen, R. L. Macklin, C. Y. Fu, and R. R. Winters, Phys. Rev. C7, (1973) 2598
18) L. R. Medsker and H. E. Jackson, Phys. Rev. C9, (1974) 709
19) H. E. Jackson and E. N. Strait, Phys. Rev. Letters 27, (1971) 1654
20) H. E. Jackson, Phys. Rev. C9,(1974) 1148 and references therein on earlier work
21) P. Axel, Phys. Rev. 126, (1962) 671
22) B. R. Mottelson, Proc. Int. Conf. on Nuclear Structure, Kinston, 1960, ed. D. A. Bromley and E. W. Vogt (University of Toronto Press, Toronto, Canada, 1960) p. 525
23) C. D. Bowman, R. J. Baglan, B. L. Berman, and T. W. Phillips, Phys. Rev. Letters 25, (1970) 1302
24) R. E. Toohey and H. E. Jackson, Phys. Rev. C6, (1972) 1440
25) J. D. Vergados, Phys. Lett. 36B, (1971) 12
26) L. M. Bollinger, Proc. Int. Conf. on Photonuclear Reactions and Applications, Asilomar , March 26-30, 1973 (USAEC Office of Information Services, Oak Ridge, Tenn.) Vol. II, p. 783
27) K. Rimawi, J. B. Garg, R. E. Chrien, G. W. Cole, and O. A. Wasson, Phy. Rev 9C (1974) 1978